Comparative Study of Slot -Entry hybrid journal Bearings

Aly. Abdelbadie[1], W.A. Crosby[2], I.M. ElFahham[3]

M. Sc. Mechanical Engineering, Engineering consultant at Alexandria Port Maritime, Egypt[1]

Professor, Mechanical Engineering Department, Faculty of Engineering, University of Alexandria, Egypt[2]

Associate Professor, Mechanical Engineering Department, Faculty of Engineering, University of Alexandria, Egypt[3]

Abstract— A theoretical study of non-recessed slot entry hybrid journal bearings with different symmetric and asymmetric geometrical configurations has been presented. Finite difference method was used to compare the performance of symmetric and asymmetric bearings considering the effect of temperature rise on viscosity. Optimum number of slots for each configuration has been studied. The results of the data presented show the optimum number of slots for each row of double row symmetric configuration and for single row asymmetric case. The results also show that, asymmetric geometric configuration has higher load carrying capacity than that of symmetric geometric configuration. The results also indicate that, the effect of temperature rise on load carrying capacity of the bearing is more pronounced in symmetric than that in asymmetric configuration. The comparative study further indicates that asymmetric geometric configurations have better stability threshold speed margin compared with symmetric geometric configurations.

Keywords — Hybrid Bearing, slot-entry, asymmetric bearing.

1 INTRODUCTION

THe Hybrid journal bearing are bearings that operate under both hydrodynamic effect and a pressurized lubricant.

Recently, hybrid journal bearings are being used to support heavy loads under high speeds. Applications of this type of bearings are found in grinding spindles, machine tool spindles, high-speed turbo machinery… etc. This kind of bearing combines the physical mechanisms of both hydrostatic and hydrodynamic bearings where both hydrostatic and hydrodynamic features are used to achieve the necessary load support. The hybrid journal bearings can be classified into two types: hole-entry hybrid bearing and slot-entry hybrid bearing as shown in Figure 1. Each type can also have a recessed or non-recessed end as illustrated in Figure 2. The non-recessed bearings are easy to manufacture, have reduced manufacturing cost and generate more hydrodynamic effect at high speeds as compared to recessed journal bearings. Therefore, in the plain hybrid bearings, the recesses in the bearing surfaces are avoided in order to maximize the hydrodynamic effect. Finally, the types of bearing's configurations can be further classified to either symmetric or asymmetric configurations these are analyzed and shown in the Mathematical Modeling section.

Many researches [1-5] concerning slot-entry journal bearings have been carried out. Satish C. Sharma et al [2, 3, 5] presented a theoretical study concerning the performance of hydrostatic and hybrid journal bearing compensated by slot restrictor. Results indicate that asymmetric slot-entry journal bearings provide an improved stability threshold speed margin compared with asymmetric hole entry journal bearings. The results further indicate that, to get optimum performance of a bearing, proper selection of the bearing parameters and type of bearing configuration are essential. Zhang [6] investigated four different types of fluid bearings: hydrodynamic, aerodynamic, hybrid fluid and bi-directional rotating fluid bearings system. He found that, for a hybrid configuration, the numerical analysis shows a decrease in power consumption. Hsien and Huang [7] studied hybrid bearings with single-row, 6 slots with orifice compensation. Results indicate that, restriction parameter and land-width ratio are substantial factors that affect the load carrying capacity and the stability of the systems. Mancilla et al [8] studied the imbalance response of a rotor supported by a hybrid bearing and that supported by a conventional hydrodynamic bearing. The results indicate that the pressurized design is capable of decreasing the vibration amplitude in most speed ranges. Therefore, it is shown clear superiority of the hybrid bearing as far as stability behavior is concerned.

Garg [9] presented a theoretical study concerning the rheological effects of the lubricant on the performance of hybrid journal bearing with asymmetric slot-entry configuration. The results show that the variation of viscosity due to rise of lubricant's temperature affects the performance quite significantly. Vikas et al [10] presented a study of the wear of a hybrid journal bearing with 2-lobe and four-pocket. The results illustrate that wear affects the performance of the bearing. Therefore the proper selection of surface roughness leads to better performance. Satish and Nathi Ramn [11] presented a study for slot-entry hybrid journal bearing with micropolar lubricants. They concluded that, the minimum film thickness in this type has a bigger value than that in the corresponding similar with Newtonian lubricant. Also, the coefficient of friction is less than that with Newtonian lubricant. Dwivedi and Kumar [12] studied the advantages and disadvantage of hybrid journal bear-

ings. Design of the hybrid bearings depends on both of the hydrodynamic effect and the hydrostatic effect to reach the required load support. Vikas et al [13] presented a comparative study for hybrid journal bearing with 2-lobe multi-recess and compensated with flow control devices. Their results indicate that, to improve the bearing performance, suitable type of compensating device should be selected.

The theoretical analysis presented in the following sections has considered the thermal effects in slot-entry hybrid journal bearing. This study illustrates a comparison of load carrying capacity as well as stability threshold for slot -entry hybrid journal bearing with symmetric and asymmetric configurations.

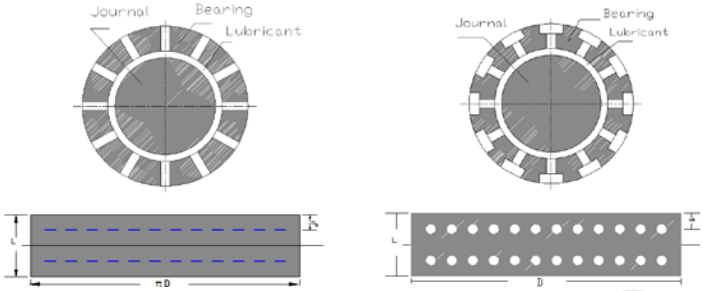

a- Slot-Entry b- Hole-Entry

Fig. 1 Types of hybrid journal bearing configurations

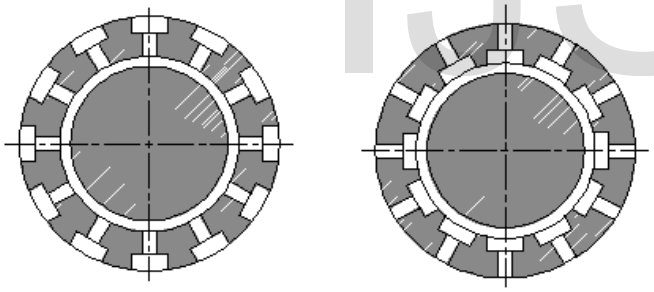

a- Non-recessed bearing b- Recessed bearing

Fig. 2 Hybrid journal bearing configurations

2 Mathematical Modeling

The analysis concerns non-recessed slot entry hybrid journal bearings with symmetric and asymmetric configurations. It started with the generalized Reynolds equation for fluid flow with variable viscosity in order to determine the pressure distribution in the space between journal and bearing. The energy equation is used to determine the temperature rise, and the 3D heat conduction equation is used to compute the temperature rise in the bush.

2.1 Bearing geometry

The bearings considered in this study have circular shape with non-recessed slot entry. For comparative analysis, different geometries are used such as symmetry and asymmetry configurations and single and double rows as shown in Figure 3 and Figure 4. The number of slots entry ranged from 4 to 24 slots per row. Different operating parameters are considered such as length to diameter ratio, eccentricity ratio, land width ratio and restrictor design parameter.

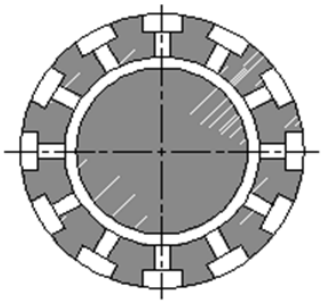

Fig. 3 Hybrid journal bearing configurations

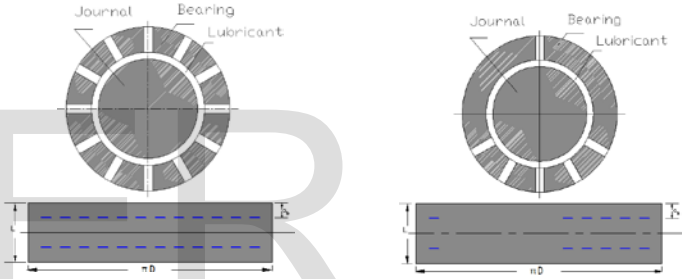

a-Symmetriccon figurations b-Asymmetric configurations

Fig. 4 Slot-Entry hybrid journal bearing configurations

2.2 Governing Equation

The co-ordinates X, Y, Z are taken in circumferential direction, across the film thickness and along the axis of the bearing respectively. The journal rotates with angular velocity as shown in Figure 5. The generalized Reynolds equation for laminar flow of incompressible fluids is the governing equation for the lubricant flow in the clearance space of journal and bearing as presented by Dowson [1] in the following form:

$$\frac{\partial}{\partial\theta}(\bar{h}^3\bar{k}_2\frac{\partial\bar{p}}{\partial\theta})+\frac{\partial}{\partial\bar{z}}(\bar{h}^3\bar{k}_2\frac{\partial\bar{p}}{\partial\bar{z}})=\Omega\frac{\partial}{\partial\theta}((1-\frac{\bar{k}_1}{\bar{k}_0})\bar{h})+\frac{\partial\bar{h}}{\partial\bar{t}} \quad (1)$$

Where the dimensionless viscosity functions $\bar{k}_0$, $\bar{k}_1$, $\bar{k}_2$ are expressed as:

$$\bar{k}_0 = \int_0^1 \frac{1}{\bar{\mu}} d\bar{y},\ \bar{k}_1 = \int_0^1 \frac{\bar{y}}{\bar{\mu}} d\bar{y},\ \bar{k}_2 = \int_0^1 \frac{\bar{y}}{\bar{\mu}} \left(\bar{y} - \frac{\bar{k}_1}{\bar{k}_0} \right) d\bar{y} \quad (2)$$

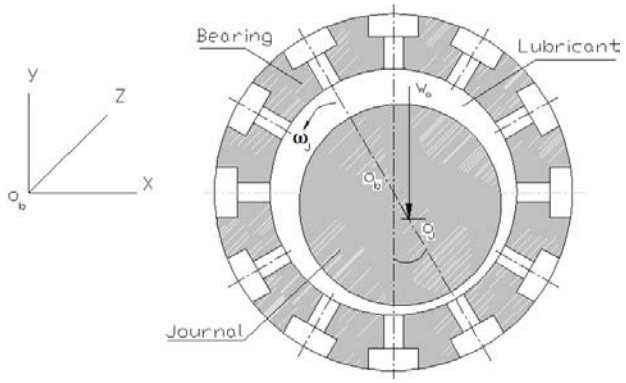

Fig. 5 Geometric details and coordinate system

The boundary conditions are assumed as:

a. All nodes on the external boundary of the bearing have zero pressure.

$$p_{(\pm L/2)} = 0.0$$

b. The restrictor flow $\bar{q_r}$ is equal to input flow of bearing at slot.

c. The pressure and its gradient in x direction at the trailing edges of the positive region equal zero.

$$p = 0.0\ ,\frac{\partial p}{\partial \theta} = 0.0 \quad (3)$$

The viscosity, which is considered to be temperature dependent, is defined in dimensionless form as [14].

$$\bar{\mu} = \frac{\mu}{\mu_0} \text{ Where } \bar{\mu} = \exp\left(-\zeta\left(T - T_0\right)\right) \quad (4)$$

The non-dimensional fluid film thickness expression for a journal bearing with reference to a fixed coordinate axis is given by the following expression:

$$\bar{h} = 1 - \bar{X}_j \cos\alpha - \bar{Z}_j \sin\alpha \quad (5)$$

2.3 Flow Equation for Restrictor

Usually, flow control devices are used with externally pressurized non-recessed journal bearings. The lubricant flow in most common flow control devices is expressed in non-dimensional form as [2]

a. Capillary $\bar{q_r} = \bar{C}_{sR}(1 - \bar{p}_r)$ (6)

b. Orifice $\bar{q_r} = \bar{C}_{sR}(1 - \bar{p}_r)^{0.5}$ (7)

c. Constant flow valve $\bar{q_r} = \bar{q_c}$ (8)

d. Slot entry restrictors $\bar{q_r} = \bar{C}_{sR}(1 - \bar{p}_r)$ (9)

Where: $\bar{p_r}$ is the dimensionless pressure at bearing slot.

$\bar{C}_{sR}$ is the slot-restrictor design parameter and is given by:

$$\bar{C}_{sR} = \frac{\pi}{36} \frac{SWR}{\lambda} \frac{k}{\bar{a}_b} \left(\frac{a_b}{Y_s} \right) \left(\frac{Z_s}{c} \right)^3 \quad (10)$$

Where:

$\bar{a}_b = a_b / L$ = land width ratio, K = number of rows of slots in a bearing.

(SWR) is the slot width ratio and is defined as the ratio between the actual slot width "a_s" and the maximum available slot width $(a_s)_{\max}$ as shown below:

$$SWR = \frac{a_s}{(a_s)_{\max}} = \frac{a_s n}{\pi D} \quad (11)$$

In the case of $\varepsilon = 0.0$, which is the concentric condition:

$\bar{\beta}^* = p^* / p_s$ = concentric design pressure ratio (the dimensionless pressure ratio at concentric condition).

$$\bar{C}_{sR} = \frac{1}{kn} \frac{\pi}{6\lambda \bar{a}_b} \left(\frac{\bar{\beta}^*}{1 - \bar{\beta}^*} \right) \quad (12)$$

2.4 Energy Equation

The energy equation in fluid film lubrication in the three dimensional mode is the result of the balance between the heat generated and the heat transferred. For an incompressible lubricant, the full 3-D energy equation which is applied to calculate the temperature in the lubricant is given as below [9]:

$$\rho C_p \left(u \frac{\partial T_f}{\partial x} + v \frac{\partial T_f}{\partial y} + w \frac{\partial T_f}{\partial z} \right) = \frac{\partial}{\partial x}\left(\alpha \frac{\partial T_f}{\partial x} \right) + \frac{\partial}{\partial y}\left(\alpha \frac{\partial T_f}{\partial y} \right) + \frac{\partial}{\partial z}\left(\alpha \frac{\partial T_f}{\partial z} \right) + \mu\psi \quad (13)$$

IJSER

Where ψ is the dissipation function and is given as follows:-

$$\psi = 2\left(\frac{\partial u}{\partial x}\right)^2 + 2\left(\frac{\partial v}{\partial y}\right)^2 + 2\left(\frac{\partial w}{\partial z}\right)^2 + \left(\frac{\partial u}{\partial y}+\frac{\partial v}{\partial x}\right)^2 + \left(\frac{\partial v}{\partial z}+\frac{\partial w}{\partial y}\right)^2 + \left(\frac{\partial w}{\partial x}+\frac{\partial u}{\partial z}\right)^2 \quad (14)$$

The fluid temperature variation is very small in the axial direction and can be neglected

$$\text{So} \quad \frac{\partial T_f}{\partial z} = 0.0 \quad (15)$$

The above energy equation (13) is reduced to the following non- dimensional form:

$$\frac{1}{p_e}\frac{\partial^2 \bar{T}_f}{\partial \bar{y}^2} + \bar{h}^2\left(\bar{u}\frac{\partial \bar{T}_f}{\partial \theta} + \frac{\bar{v}}{\bar{h}}\frac{\partial \bar{T}_f}{\partial \bar{y}}\right) - \bar{u}\,\bar{y}\,\bar{h}\frac{\partial \bar{h}}{\partial \theta}\frac{\partial \bar{T}_f}{\partial \bar{y}} + \bar{\mu}\left(\left(\frac{\partial \bar{u}}{\partial \bar{y}}\right)^2 + \left(\frac{\partial \bar{w}}{\partial \bar{y}}\right)^2\right) = 0.0 \quad (16)$$

Boundary conditions:

The boundary conditions that are necessary to solve the energy equation (16) are:-

a. On the fluid-film journal interface

$$\bar{T}_f = \bar{T}_j \qquad \text{at } \bar{y} = 1.0 \quad (17)$$

b. On the fluid-film bush interface

$$\bar{T}_f = \bar{T}_b \qquad \text{at } \bar{y} = 0.0 \quad (18)$$

2.4.1 Heat conduction equation

The temperature distribution in the bush is determined by 3-D Fourier heat conduction equation. This equation in cylindrical coordinates in a non- dimensional form is given as:

$$\frac{1}{\bar{r}}\frac{\partial}{\partial \bar{r}}\left(\bar{k}_b\,\bar{r}\frac{\partial \bar{T}_b}{\partial \bar{r}}\right) + \frac{1}{\bar{r}^2}\frac{\partial}{\partial \theta}\left(\bar{k}_b\frac{\partial \bar{T}_b}{\partial \theta}\right) + \bar{r}\frac{\partial}{\partial \beta}\left(\bar{k}_b\frac{\partial \bar{T}_b}{\partial \beta}\right) = 0.0 \quad (19)$$

Boundary conditions:

The thermal boundary conditions for the solution of equation (19) are expressed as follows:

a. at the fluid-bush interface $\bar{y} = 0.0, \quad \bar{r} = \bar{R}_1$

$$-k_b\left(\frac{\partial \bar{T}_b}{\partial \bar{r}}\right)_{r=R_1} = \frac{k_f}{\bar{c}\,\bar{h}}\left(\frac{\partial \bar{T}_f}{\partial \bar{y}}\right)_{\bar{y}=0.0} \quad (20)$$

b. On the outer faces of the bush $\bar{r} = \bar{R}_2$ the free convectiongives:

c. $$-\left(\frac{\partial \bar{T}_b}{\partial \bar{r}}\right)_{\bar{r}=R2} = -\frac{h_b R}{k_b}\left(\bar{T}_b\,|_{\bar{r}=R2} - \bar{T}_a\right) \quad (21)$$

d. On the lateral faces of the bearing $\beta = \pm L/2$

$$\left(\frac{\partial \bar{T}_b}{\partial \beta}\right)_{\beta=\pm L/2} = -\frac{h_b R}{k_b}\left(\bar{T}_b\,|_{\beta=\pm L/2} - \bar{T}_a\right) \quad (22)$$

e. At the inlet edge of the supply slots, the temperature ($\bar{T}_b$) is assumed to be equal to the oil supply temperature ($\bar{T}_s$).

2.4.2 Journal temperature

Due to the continuous rotation of journal, it is assumed that its temperature is uniform in the circumferential direction. In the case of thermal equilibrium, the heat flow to the journal equals to the heat flow from the journal. The amount of heat received by the journal is given by:

$$\bar{q}_{j|_{in}} = \int_{L/1}^{+L/2}\int_{0}^{2\pi} \frac{k_f R_j}{\bar{c}\,\bar{h}}\,\Big|_{y=1}\, d\theta\, d\beta \quad (23)$$

And the heat rejected through the two ends of the journal is given by

$$\bar{q}_{j|o} = \frac{2h_j A_j}{R_j}\left(\bar{T}_j - \bar{T}_a\right) \quad (24)$$

Then the journal temperature ($\bar{T}_j$) can be obtained by equating equations (23) and (24).

IJSER

Table 1 Bearing Data

Parameter	symbol	Value	Units
Bearing length	L	100	mm
journal radius	r	50	mm
Radial clearance	c	0.05	mm
Land width ratio	a_b / L	0.25	
Density	ρ	850	$kg.m^{-3}$
Specific heat of fluid	C_p	2000	$J.kg^{-1}.K^{-1}$
Thermal conductivity of fluid	k_f	0.125	$W.m^{-1}.K^{-1}$
Thermal conductivity of bush	k_b	50	$W.m^{-1}.K^{-1}$
Viscosity	μ	0.0277	Pa.s
viscosity index coefficient	ζ	0.01	
Journal speed	N	2500	rpm
External load	W_o	22.4	kN
Supply pressure	p_s	$9*10^6$	$N.m^{-2}$
Supply temperature	T	40	c^o
Ambient temperature	T_a	40	c^o

2.5 Stability parameters

It is assumed that, there is a very small disturbance for the center of the journal from its equilibrium position. The equation of motion for the journal center can be given in the non-dimensional form as:

$$\left[\bar{M}_J\right]\left\{\ddot{\bar{X}}_J\right\}+\left[\bar{C}\right]\left\{\dot{\bar{X}}_J\right\}+\left[K\right]\left\{\bar{X}_J\right\}=0.0 \tag{25}$$

By solving equation (25), the stability margin of the system for the critical mass $(\bar{M}_c)$ can be obtained.

If $\bar{M}_J < \bar{M}_c$ then, the system is stable.

Then, the dimensionless threshold speed of the journal is obtained from:

$$\bar{\omega}_{th}=\left[\bar{M}_c/\bar{W}_0\right]^{0.5} \tag{26}$$

Where, $(\bar{W}_0)$ is the reaction force at $\left(\frac{\partial \bar{h}}{\partial \bar{t}}=0.0\right)$

3 Results and Discussions

The design of a hybrid bearing depends on many parameters that affect the bearing performance such as length to diameter ratio, eccentricity ratio, land width ratio…..etc. Therefore, this comparative study is important for the selection of the suitable type of bearing configuration. The representative values have been computed according to lubricant's properties, operating and geometric parameters of the bearing as shown in Table 1.

Figure 6 shows the relation between slot-restrictor design parameter and the dimensionless maximum pressure in both isothermal and thermo-hydrodynamic cases. The figure illustrates the relation for the case of double rows with 6 slots in each row with symmetric and asymmetric configurations. It is found that the maximum dimensionless pressure is reduced in the thermo-hydrodynamic cases. Figure 7 shows the relation between slot-restrictor design parameter and the dimensionless load carrying capacity in both isothermal and thermo-hydrodynamic cases. It is indicated that the load carrying capacity is reduced in the thermo-hydrodynamic cases. Figure 8 illustrates the variation of dimensionless load carrying capacity versus eccentricity ratio for bearings with symmetric configuration. It is found that a bearing with double rows and 6 slots /row gives higher load carrying capacity than that having a single row and 12 slots. Figure 9 and Figure 10 illustrate the variation of the dimensionless load carrying capacity versus eccentricity ratio for a single row with 6 and 8 slots. It is shown that the case of an asymmetric configuration gives better load carrying capacity than in the case of symmetric configuration. Fig. 11 shows this relation for symmetric and asymmetric configurations with double rows and 12 slots each. The results show that asymmetric configuration gives

higher load carrying capacity than symmetric configuration.

In the above mentioned comparison of load carrying capacity, it is found that, the hydrodynamic effect in the asymmetric configuration becomes higher than that in symmetric configuration. Hence the load carrying capacity becomes higher.

The variation in dimensionless load carrying capacity in the isothermal and thermo-hydrodynamic cases is presented in Figure 12. It is shown that the cases of asymmetric configurations give higher load carrying capacity than the symmetric configurations for both isothermal and thermo-hydrodynamic cases. It is also shown that for the same configurations the

IJSER

load carrying capacity in isothermal cases is higher than that in thermo-hydrodynamic cases. The relation between the number of slots per row and the load carrying capacity at eccentricity ratio e = 0.7 is shown in Figure 13 for the symmetric case and is shown in Figure 14 for the asymmetric case. It is clear that the optimum number of slots per row for the case of symmetry with double rows is 12 slots. It is also found that the optimum number of slots per row for the case of asymmetry with single row is 6 slots. Figure 15 illustrates the changes of threshold speed ($\bar{\omega}_{th}$) due to the variation of the speed parameter (Ω) for both the symmetric and asymmetric configurations. The region below the curves is stable while the region above the curves is unstable. It is clear that, the bearing with asymmetric configuration is slightly more stable than that of symmetric configuration.

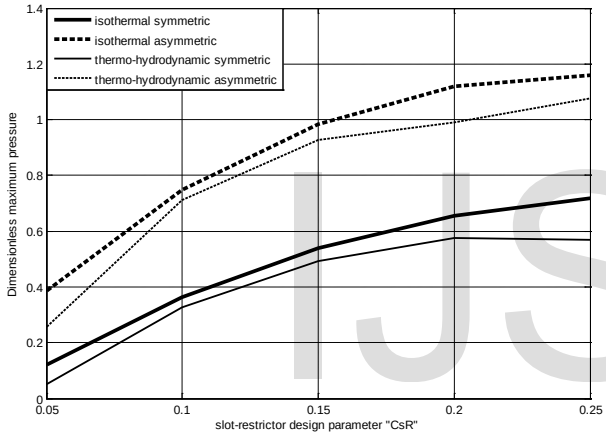

Fig. 6 Variation of dimensionless maximum pressure vs. slot-restrictor design parameter for different configurations for thermo-hydrodynamic and isothermal cases

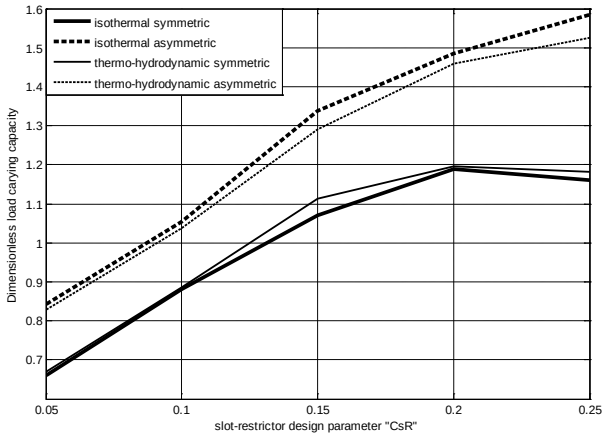

Fig. 7 Variation of dimensionless load carrying capacity vs. slot-restrictor design parameter for different configurations for thermo-hydrodynamic and isothermal cases

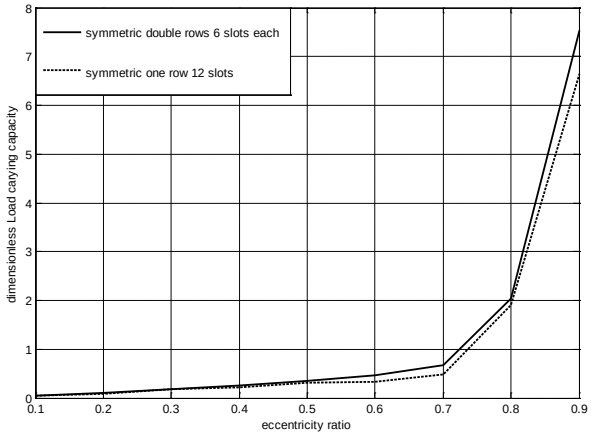

Fig. 8 Variation of dimensionless load carrying capacity vs eccentricity ratiofor symmetric configuration for single row 12 slots, and double rows 6 slots each

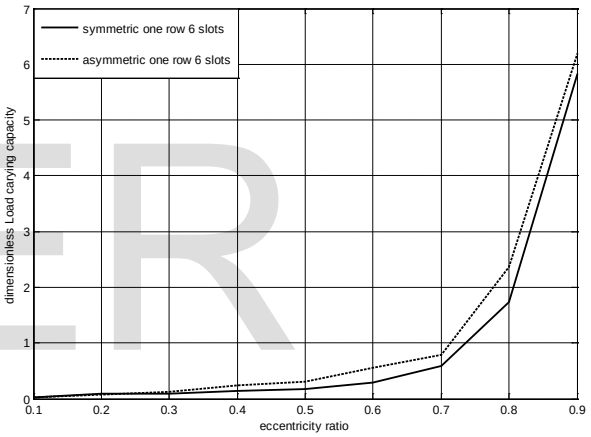

Fig. 9: Variation of dimensionless load carrying capacity vs eccentricity ratio for symmetric and asymmetric configurations with single row and 6 slots

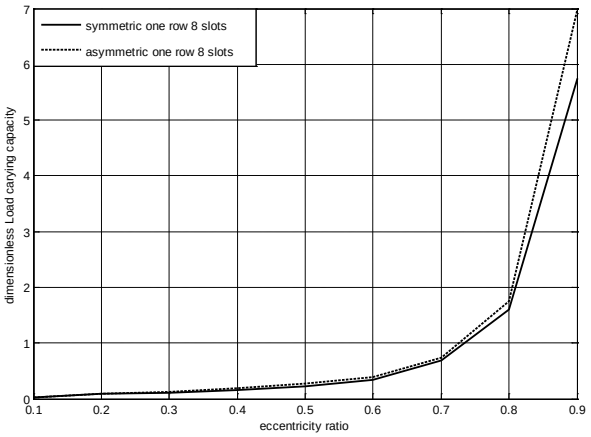

Fig. 10: Variation of dimensionless load carrying capacity vs eccentricity ratio for symmetric and asymmetric configurations with single row and 8 slots

IJSER

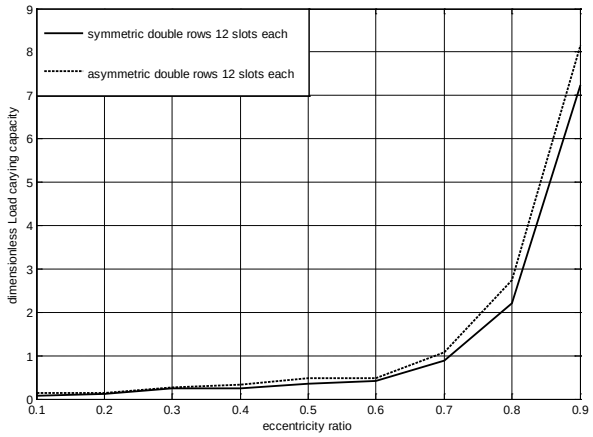

Fig. 11 Variation of dimensionless load carrying capacity vs centricity ratiofor symmetric and asymmetric configurations ith double row and 12 slots each

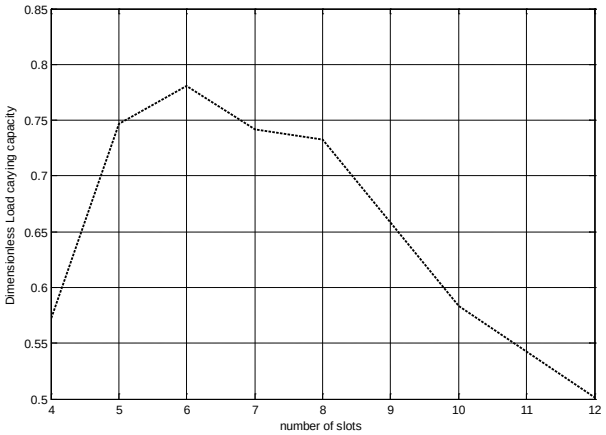

Fig. 14: number of slots vs load carrying capacity for single row asymmetry configuration

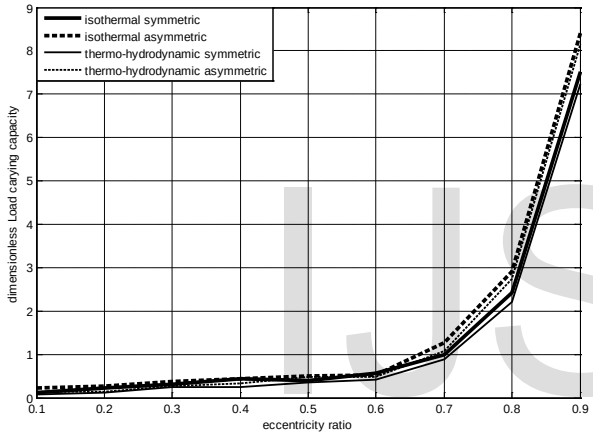

Fig. 12 Variation of dimensionless load carrying capacity vs eccentricity ratio with different configurations for thermo-hydrodynamic and isothermal cases

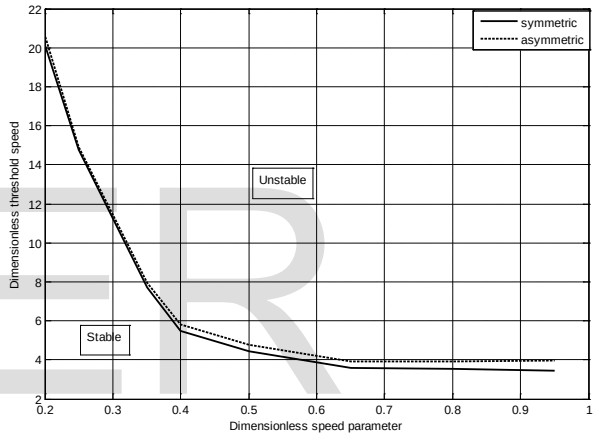

Fig. 15 Variation of stability threshold speed margin

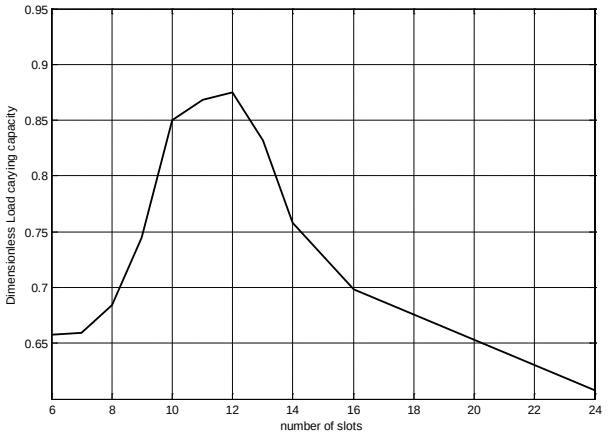

Fig. 13: number of slots vs load carrying capacity for double rows symmetry configuration

4 CONCLUSION

An analytical comparative study of the different configurations of the slot-entry hybrid journal Bearings has been carried out. It was concluded that:

a. Considering the load carrying capacity, the asymmetric configuration of slot-entry hybrid bearing gives a better performance than that of the symmetric configuration for the same eccentricity ratio.

b. In the case of symmetry configuration, the optimum load carrying capacity is attained using double rows with 12 slots per row, while it is attained with single row 6 slots for asymmetry configuration.

c. From the stability point of view, it is observed that the slot-entry hybrid journal bearing with asymmetric configuration is slightly more stable than that with symmetric configuration.

IJSER

NOMENCLATURE

DIMENSIONAL PARAMETERS

A : Area (m^2)

ab: Axial land width (m)

as: Extent of slot (m)

ζ : Viscosity index coefficient

C_{ij} : Fluid-film damping coefficients ($N.m^{-2}$)

D: Journal diameter (m)

e: Journal eccentricity (m)

h: Fluid-film thickness (m)

h_b: Heat transfer coefficient for the bush ($W.m^{-1}.K^{-1}$)

k_b: Thermal conductivity for the bush ($W.m^{-1}.K^{-1}$)

k_f: Thermal conductivity for the fluid ($W.m^{-1}.K^{-1}$)

M : Mass (kg)

N : Rotational speed (rpm)

p : Pressure ($N.m^{-2}$)

p_s: Supply Pressure ($N.m^{-2}$)

p^*: Pressure at concentric condition i.e at $\varepsilon = 0.0$.

R_1, R_2: Inner and outer bush radius (m)

r: Radial coordinate

Sij: Fluid-film stiffness coefficients (*i, j* = x, y) ($N.m^{-1}$)

t : Time $(\sec.)$

T : Temperature C^0

T_a: Ambient temperature C^0

($W.m^{-1}.K^{-1}$)

M : Mass (kg)

N : Rotational speed (rpm)

p : Pressure ($N.m^{-2}$)

p_s: Supply Pressure ($N.m^{-2}$)

p^*: Pressure at concentric condition i.e at $\varepsilon = 0.0$.

R_1, R_2: Inner and outer bush radius (m)

r: Radial coordinate

Sij: Fluid-film stiffness coefficients (*i, j* = x, y) ($N.m^{-1}$)

t : Time $(\sec.)$

T : Temperature C^0

T_a: Ambient temperature C^0

NON-DIMENSIONAL PARAMETERS

$\bar{a}_b$: Land width ratio $= a_b / L$

$\bar{q}_{j\backslash in}$: Heat flow to the journal

$\bar{q}_{j\backslash o}$: Heat flow from the journal

$\bar{\beta}^*$: Concentric design pressure ratio $= p^* / p_s$

$\bar{p}$:Dimensionless pressure $= p / p_s$

λ : Ratio of (L/D)

n: Number of slots,

ε: Eccentricity ratio = e / c

$\bar{T}$: Dimensionless temperature $= (T - T_0) / T_0$

$\bar{y}$: Dimensionless Coordinate along film

p_e :Peclet number $= (\rho C_p \omega c^2) / \alpha$

$\bar{h}$: Dimensionless fluid-film thickness $= h / c$

$\bar{\mu}$: Dimensionless viscosity $= \mu / \mu_0$

$\bar{k}_b$: Dimensionless thermal conductivity for the bush $= k_b / k_r$

$\bar{T}_b$: Dimensionless bush temperature $= T_b / T_0$

$\beta = z / r_j$,

$\theta = x / r \quad , \quad \bar{z} = z / L \qquad \Omega = \omega(\mu_r r^2) / (c^2 p_s)$

IJSER

5 References

[1] Dowson D, "A generalized Reynolds equation for film fluid lubrication". Int. Journal Mech. Sc. Pergamon Press. Vol. 4, pp. 159 -170, 1962.

[2] Satish C. Sharma , Vijay Kumar, S.C. Jain, R. Sinhasan, "A study of slot-entry hydrostatic/hybrid journal bearing using the finite element method", Tribology International 32 (1999) 185–196.

[3] Satish C. Sharma, S.C. Jain, N. Madhu Mohan Reddy," Influence of elastic effects on the performance of slot- entry journal Bearings", Tribology International 32 (1999) 537–551

[4] H. Hirani, K. Athre, S. Biswas, "a Hybrid solution scheme for performance evaluation of crankshaft bearings", Journal of Tribology, Vol.122/733(2000).

[5] Satish C. Sharma, Vijay Kumar, S.C. Jain, T. Nagaraju, Giriraj Prasad," Thermo hydrostatic analysis of slot- entry hybrid journal bearing". Tribology International 35 (2002) 561–577.

[6]Zhang Qide," Fluid bearing spindles for data storage devices", a thesis, National University of Singapore, 2003.

[7] Cheng-Hsien Chen, Ching-Chu Huang, "The influences of orifice restriction and journal eccentricity on the stability of the rigid rotor-hybrid bearing system", Tribology International 37 (2004) 227– 234.

[8] Julio Gomez-Mancilla, Valeri Nosov, Gerardo Silva-Navarro, "Rotor-bearing system stability performance comparing hybrid versus conventional bearings". International Journal of Rotating Machinery 2005:1, 16–22.

[9]H. C. Garg, "Performance of asymmetric slot-Entry hybrid journal bearing operating with non- newtonian Lubricant", Journal of Engineering and Technology, Jan-Jun 2011 Vol 1 Issue 1.

[10]Vikas M.Phalle, Satish. Sharma, S.C.Jain," Influence of wear on the performance of a 2-lobe multirecess hybrid journal bearing system compensated with membrane restrictor", Tribology

international l44 (2011) 380–395.

[11] Satish C. Sharma, Nathi Ram, "Influence of micropolar lubricants on the performance of slot-entry hybrid journal Bearing", Tribology International 44 (2011) 1852–1863.

[12] V. K. Dwivedi, Sanjeev Kumar Gupta, "Finite Difference Method Analysis of Hybrid Bearing", Proc. of the 5thInternationalConference on Advances in Mechanical Engineering (ICAME-2011), June 06-08,

2011.

[13]Vikas M.Phalle, Satish C.Sharma, S.C.Jain, "Performance analysis of a 2-lobe worn multi recess hybrid journal bearing system using different flow control devices". Tribology International 52 (2012) 101–116.

[14] Prashant .Kushare, Satish C.Sharma. "A study of 2-lobe symmetric hole entry hybrid journal bearing operating with non-Newtonian lubricant considering thermal effects", Tribology International 92(2015)567–576.

IJSER